Eur Radiol (2006) 16: 1651–1658
DOI 10.1007/s00330-006-0175-8

Thierry A. G. M. Huisman
Thomas Loenneker
Gerd Barta
Matthias E. Bellemann
Juergen Hennig
Joachim E. Fischer
Kamil A. Il'yasov

Quantitative diffusion tensor MR imaging of the brain: field strength related variance of apparent diffusion coefficient (ADC) and fractional anisotropy (FA) scalars

Received: 27 June 2005
Revised: 22 December 2005
Accepted: 20 January 2006
Published online: 11 March 2006

This paper was presented at the 21st Annual Scientific Meeting of the ESMRMB, September 9–12, 2004, Copenhagen, Denmark

T. A. G. M. Huisman (✉) · T. Loenneker · K. A. Il'yasov
Department of Diagnostic Imaging, University Children's Hospital Zurich, Steinwiesstrasse 75, 8032 Zurich, Switzerland
e-mail: thierry.huisman@kispi.unizh.ch
Tel.: +41-1-2667110
Fax: +41-1-2667158

G. Barta · J. Hennig · K. A. Il'yasov
Department of Diagnostic Radiology, Section of Medical Physics, University of Freiburg, Freiburg, Germany

G. Barta · M. E. Bellemann
Department of Medical Engineering, University of Applied Sciences Jena, Jena, Germany

J. E. Fischer
Growth and Development Center, University Children's Hospital Zurich, Zurich, Switzerland

Abstract The objectives were to study the "impact" of the magnetic field strength on diffusion tensor imaging (DTI) metrics and also to determine whether magnetic-field-related differences in T2-relaxation times of brain tissue influence DTI measurements. DTI was performed on 12 healthy volunteers at 1.5 and 3.0 Tesla (within 2 h) using identical DTI scan parameters. Apparent diffusion coefficient (ADC) and fractional anisotropy (FA) values were measured at multiple gray and white matter locations. ADC and FA values were compared and analyzed for statistically significant differences. In addition, DTI measurements were performed at different echo times (TE) for both field strengths. ADC values for gray and white matter were statistically significantly lower at 3.0 Tesla compared with 1.5 Tesla (% change between −1.94% and −9.79%). FA values were statistically significantly higher at 3.0 Tesla compared with 1.5 Tesla (% change between +4.04 and 11.15%). ADC and FA values are not significantly different for TE=91 ms and TE=125 ms. Thus, ADC and FA values vary with the used field strength. Comparative clinical studies using ADC or FA values should consequently compare ADC or FA results with normative ADC or FA values that have been determined for the field strength used.

Keywords Diffusion tensor imaging · Apparent diffusion coefficient · Fractional anisotropy · Magnetic field strength

Introduction

Since its introduction in the late 1980s, diffusion weighted magnetic resonance imaging (DWI) has become an important diagnostic tool in neuroradiology [1–4]. DWI has proven to be especially valuable in the early detection of hyperacute cerebral ischemia [5–7] as well as in many other neurological disorders [8–18].

With the development of diffusion tensor imaging (DTI) the three dimensional shape and the magnitude of diffusive water motion within the brain can be measured [19]. Although the determinants of water diffusion are not yet fully understood, it is generally agreed that the microstructural architecture of the brain tissue mainly determines the shape and magnitude of the diffusion tensor. Additional factors that determine the diffusion tensor include physico-

chemical tissue properties, active transport mechanisms, as well as tissue perfusion dynamics [20, 21]. DTI sequences with calculation of apparent diffusion coefficient (ADC) and fractional anisotropy (FA) scalars allow characterization of the shape and magnitude of the diffusion ellipsoid. These parameters consequently reflect the microstructural architecture of the brain. For clinical use, these scalars can be used for comparison between individual patients, for serial examinations in the same patient and for the evaluation of normal and pathological cerebral maturation during childhood. In addition, quantification of diffusion can be especially helpful as it may allow early diagnosis of pathology. Many disease processes start at the microstructural level, which change the three-dimensional (3D) shape of water diffusion before the overall diffusion rate changes [7, 20, 22].

Many studies compare measured ADC and FA values in patients with previously published normative ADC and FA values that have been determined in healthy children and adults on a 1.5-Tesla magnetic resonance imaging (MRI) units [23–26]. With the increasing availability of higher field strength MR units (e.g., 3 Tesla) an increasing number of clinical studies will measure ADC and FA values at higher field strengths. Consequently, it is of essential importance to know if DTI scalars vary with field strength. The need for comparative studies evaluating the impact of field strength on ADC and FA measurements is obvious. Theoretically, ADC and FA values should be independent of the used field strength because water diffusion is not influenced by the magnetic field. However, the few studies of this topic showed partially contradictory findings. One recent study comparing 1.5 and 3 Tesla in a series of seven healthy volunteers concluded that the mean diffusivity and FA did not differ significantly [27], while, on the other hand, in several phantom studies an inverse relationship between field strength and ADC of cerebral metabolites was seen [28]. In addition, shorter T2 relaxation times at higher field strengths have also been discussed to influence DTI scalars [28].

The goals of our study were (1) to compare ADC and FA values measured at 1.5 and 3.0 Tesla using DTI sequences that are as identical as possible and (2) if magnetic-field-related differences in T2-relaxation times of brain tissue may explain differences in DTI scalars.

Materials and methods

Twelve healthy volunteers (ten men, two women; age range, 26–31 years; median age 28 years) without a history of neurologic or other systemic diseases were examined at 1.5- and 3-Tesla MRI units within 2 h. The local ethics committee had approved the study. Informed consent was obtained in all volunteers. Individuals were allocated in a random manner to be investigated with 1.5 Tesla or 3.0 Tesla first.

DTI was performed on a 1.5 Tesla (Magnetom Sonata; Siemens Medical Systems, Erlangen, Germany) and a 3.0 Tesla (Magnetom Trio, Siemens Medical Systems, Erlangen, Germany). Both scanners are equipped with identical gradient hard- and software and are capable of a maximal gradient strength of 40 mT/m. Imaging was acquired with a standard circularly polarized radio-frequency head coil. Prior to DTI measurement, a 3D T1-weighted MPRAGE sequence was acquired with an isotropic 1 mm^3 spatial resolution. Axial slices according to an imaging plane parallel to the anterior-posterior commissure connecting line were reformatted from the 3D data set. The diffusion tensor was sampled by repeating a diffusion-weighted single-shot spin-echo echo-planar sequence along 12 different geometric directions. Diffusion sensitization was achieved by using two balanced, bipolar diffusion gradients centered around the 180° radiofrequency pulse. To reduce eddy current effects, the diffusion gradients were divided into four alternating-sign gradient lobes, all with the same gradient magnitude [29]. An effective b-value of 1,000 mm^2/s was used for each of the 12 diffusion encoding directions. An additional measurement without diffusion weighting (b=0 mm^2/s) was performed to allow calculation of the ADC values. Scan parameter were identical for both scanners to ensure comparability: repetition time (TR) 8,000 ms, echo time (TE) 91 ms, matrix size 128×120, field of view 256×240 mm. The resulting in-plane resolution was 2×2 mm. A total of 51 contiguous 3-mm thick axial slices were acquired covering the brain from the skull base to the vertex. Positioning of the axial DTI slices were copied from the reconstructed axial T1-weighted MPRAGE slices to assure identical imaging planes for all DTI measurements. Each diffusion tensor was sampled six times to optimize the signal-to-noise ratio (SNR). The Siemens pulse sequence simulation tool was applied to prove that the DTI pulse sequences were identical on both scanners. Gradient shapes generated with the stimulation tool were used for exact numerical b-tensor calculation. Due to intrinsic contrast variations by diffusion encoding along the 12 different geometric directions a “common” motion correction is not possible. Instead special care was taken to minimize head motion by restraining the subject’s head with tightly packed cushions and a proper instruction by the operator. In addition, the residual error of the fit was controlled and b_0-images were also checked for motion. The imaging protocol for the phantom measurements was identical to that for the volunteers.

In six volunteers, DTI was performed with two different echo times (TE=91 and 125 ms) to evaluate the impact of magnetic field related differences in T2-relaxation on the quantitative DTI measurements. With the exception of the echo times, all other imaging parameter were kept identical. The effect of changes in the duration, amplitude and separation of the diffusion gradients on the b-value was controlled by an accurate b-matrix calculation. The b-

matrix was calculated numerically on the basis of the exact gradient shapes of all gradients (diffusion encoding and imaging gradients) [30]. The b-matrix changed slightly, which was taken into account in the calculations. The potential effect of a slightly different diffusion time on the measured apparent diffusion tensor is minimal and could consequently be ignored.

A water phantom was used for calibration of the gradient amplitudes and verification of the quantitative diffusion measurements. Measured ADC values were compared with previously published data after correction for the sample temperature [26, 31].

ADC values were calculated on a pixel-by-pixel basis using a two-point (b=0 and b=1,000 mm^2/s) monoexponential fit approach. Fractional anisotropy maps were calculated as the ratio of the anisotropic component of the diffusion tensor to the whole diffusion tensor as previously published by Basser and Pierpaoli [32].

For data analysis, the reconstructed maps were transferred to a personal computer. Quantitative analysis was performed by outlining regions of interest (ROIs) using homemade routines (KI) based on commercially available image display software (Matlab 6.5). ROIs were manually placed by an experienced neuroradiologist (T.H.) at the following seven anatomical locations: genu of the internal capsule; posterior limb of the internal capsule; centrum semiovale; thalamus; head of the caudate nucleus; splenium and truncus of the corpus callosum (Fig. 1). With the exception of the corpus callosum, all ROIs were positioned bilaterally. The five bilateral measurements were averaged for each location. ROI positioning was primarily performed on the FA maps. The high gray-white matter discrimination facilitates the identification of the anatomical margins of the different structures. The correct ROI positioning was checked and where necessary corrected by means of ROI overlay onto the corresponding ADC maps. Care was taken to minimize ROI contamination by partial volume effects of adjacent structures. Identical ROI placement on the ADC and FA maps was achieved by using a copy-paste tool of the ROIs.

The SNR was estimated for both field strengths. The SNR was calculated from the averaged T2-weighted, b_0-images as the ratio between the mean signal intensity of a 5×5 pixel ROI positioned within the thalamus and the standard deviation of the noise measured in background areas outside of the head that were free of artifacts [7]. These ROIs were positioned along the direction of the frequency encoding gradients to avoid contamination by signals originating from "ghosts" along the phase-encoding gradient direction.

Statistical analysis was carried out with the mean ADC and FA values and their standard deviations of each ROI as the raw data. The rational for using mean ADC and FA values and their standard deviations was the assumption that within repeated measures of the same region any intra-individual differences would represent stochastic measurement error and, therefore, would follow a normal distribution. In contrast, we did not assume a priori that between-subject differences or between-method differences would necessarily follow a normal distribution. Therefore, the distribution of the individual's mean ADC and FA was assessed from reviewing normality plots, skewness and kurtosis. Data were compared using the paired *t*-test for variables approximating a normal distribution. As most of the data reasonably approximated a normal distribution, we present the means and the standard deviations. We repeated all group comparisons using the Wilcoxon signed rank test and present these findings as additional results where appropriate. Finally, a repeated measures MANOVA was carried out with the repeated measures factor method (1.5 vs 3 Tesla) and the second factor LOI to test for main effects of method. A *P* value of less than 0.05 was considered to indicate statistically significant differences. All calculations were carried out using SPSS (version 12; SPSS, Chicago, Ill.).

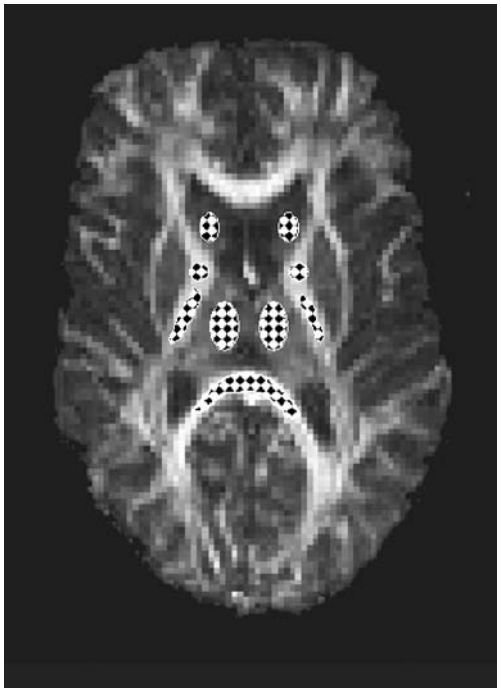

Fig. 1 Axial FA map of the cerebrum with a sample of superimposed ROIs as used for data analysis [Genu internal capsule, posterior limb internal capsule, thalamus, caput caudate nucleus (all bilateral) and splenium corpus callosum]

Results

All images were of good image quality. No motion was detected for any of the measurements, no misregistration or image warping due to eddy current distortion with artifactual anisotropy was observed. On qualitative inspection, both ADC and FA maps appeared similar for both field strengths. There was essentially no gray-white matter

contrast visible on the ADC maps, while a strong gray white matter contrast was seen on the FA maps. Densely packed white matter tracts with high degrees of anisotropy could, consequently, easily be discriminated from the isotropic gray matter (Fig. 1).

Calibration measurements on both scanners were in good agreement with data from the literature [33]. The difference between the "literature" ADC values interpolated to the temperature of the phantom and the measured ADC values was less than 2%. The difference between the ADC values measured on the two scanners, interpolated to 20°C, was also less than 2%. Since the SNR of b_0-images of a phantom was around 200, the expected ADC variation due to the noise was around 2% [31]. Consequently, the observed differences between the two scanners were in the range of accuracy of the calibration measurements.

We did not detect any differences in gradient calibrations for the X, Y and Z channels; the ADC values measured along these directions were the same on both scanners. The FA values measured in the water phantom were equal for both scanners, FA=0.03±0.01.

The ADC values showed a statistically significant decrease ($P<0.05$) comparing 1.5 with 3.0 Tesla ranging between −1.94 and −9.79% ADC change (Table 1). ADC values decreased in 4/7 (57%) ROIs. The largest statistically significant decrease was computed for the splenium of the corpus callosum (−9.79%); the smallest decrease for the centrum semiovale (−1.94%). The mean decrease for the white matter is −5.25%, for the gray matter −4.65%. The highest overall ADC value was computed for the central gray matter of the caput of the caudate nucleus (795×10^{-6} mm^2/s); the lowest ADC value for the white matter tracts within the splenium of the corpus callosum (653×10^{-6} mm^2/s).

In contrast to the observed ADC decrease, a statistically significant FA increase was seen for 5/7 (71%) ROIs (Table 1). The change in FA values ranged between 4.04 and 11.15%. The largest statistically significant increase was computed for the truncus of the corpus callosum (13.29%); the smallest increase for the truncus of the corpus callosum (4.78%). The mean increase for the white matter is 5.05%; for the gray matter 11.15%. The highest degree of anisotropy was computed for the tightly packed white matter tracts within the splenium of the corpus callosum (0.80); the lowest degree of anisotropy for the central gray matter of the caput of the caudate nucleus (0.17).

Multivariate analysis confirmed a main effect for field strength for ADC values (within subjects effects, Greenhouse-Geisser corrected $F_{GG}=8.36$, $df=1/10$, $P=0.016$), but not for an interaction between field and location ($F_{GG}=1.37$, $df=6/60$, $P=0.14$). The FA-values showed significant main effects for field strength ($F_{GG}=15.7$, $df=1/10$, $P=0.003$) and a trend for the interaction between field strength and location ($F_{GG}=2.34$, $df=6/60$, $P=0.09$).

Quantitative ADC and FA data measured at different echo times (TE=91 and TE=125 ms) are summarized in Tables 2, 3. No statistically significant differences in ADC and FA values were observed comparing the different echo times, neither at 1.5- nor at 3.0-Tesla field strength.

The SNR showed an averaged boost of 19.6% when comparing 1.5 with 3 Tesla.

Discussion

Diffusion tensor imaging has become a vital imaging tool in the evaluation of the brain. Diffusion tensor imaging gives qualitative and quantitative information previously not available with conventional MRI. The most widely used diffusion scalars include apparent diffusion coefficients that quantifies the netto translational water motion in the brain, and fractional anisotropy that quantifies the degree of anisotropic diffusion in the brain. The degree of anisotropic diffusion gives quantitative information about the directionality and integrity of white matter tracts. ADC and FA measurements are frequently used as biomarkers of the degree of tissue injury in brain diseases. Recent reports have established age correlated normative ADC and FA values at 1.5 Tesla MRI units [26]. In addition, a number of

Table 1 ADC and FA values measured at 1.5 and 3.0 Tesla at various white and gray matter locations. ADC×10^{-6} mm^2/s; FA are unitless, varying between 0 (maximal isotropic diffusion) and 1 (maximal anisotropic diffusion). Data are presented as mean ± standard deviation. Comparisons were made using the *t*-test for paired samples. A *P* value less than 0.05 was considered to indicate statistically significant difference

	ADC				FA			
	1.5 Tesla	3.0 Tesla	*P* value	% change	1.5 Tesla	3.0 Tesla	*P* value	% change
Genu internal capsule	701 (±29)	697 (±33)	0.58	−0.54	0.700 (±.035)	0.715 (±0.047)	0.33	2.18
Posterior limb internal capsule	713 (±19)	684 (±28)	<0.001	−4.02	0.681 (±.031)	0.722 (±0.024)	0.002	6.02
Splenium corpus callosum	724 (±18)	653 (±41)	<0.001	−9.79	0.764 (±.021)	0.800 (±0.034)	<0.001	4.78
Truncus corpus callosum	775 (±54)	781 (±34)	0.55	0.84	0.720 (±.008)	0.748 (±0.019)	<0.001	4.04
Centrum semiovale	701 (±18)	687 (±23)	0.02	−1.94	0.572 (±.022)	0.602 (±0.026)	<0.001	5.36
Thalamus	751 (±17)	717 (±27)	<0.001	−4.65	0.296 (±.062)	0.330 (±0.072)	<0.001	11.15
Caput caudate nucleus	783 (±75)	795 (±94)	0.58	−1.53	0.171 (±.032)	0.187 (±0.027)	0.90	9.37

Table 2 ADC and FA values measured at 1.5 Tesla using two different echo times (TE=91 ms and TE=125 ms). ADC×10^{-6} mm^2/s; FA are unitless, varying between 0 (maximal isotropic diffusion) and 1 (maximal anisotropic diffusion). Data are presented as mean ± standard deviation. A *P* value less than 0.05 was considered to indicate statistically significant difference

1.5 Tesla	ADC				FA			
	TE=91	TE=125	*P* value	% change	TE=91	TE=125	*P* value	% change
Genu internal capsule	719 (±25)	707 (±38)	0.51	−1.55	0.702 (±0.028)	0.690 (±.030)	0.43	−1.65
Posterior limb internal capsule	721 (±20)	724 (±11)	0.67	0.37	0.701 (±0.023)	0.706 (±.025)	0.58	0.75
Splenium corpus callosum	725 (±9)	672 (±17)	0.20	−7.30	0.825 (±0.021)	0.850 (±.016)	0.17	3.07
Truncus corpus callosum	779 (±75)	787 (±44)	0.87	1.03	0.776 (±0.031)	0.774 (±0.020)	0.95	−0.21
Centrum semiovale	709 (±13)	703 (±19)	0.32	−0.89	0.622 (±0.071)	0.603 (±0.043)	0.37	−3.19
Thalamus	766 (±14)	763 (±16)	0.58	−0.34	0.316 (±0.019)	0.327 (±0.019)	0.25	3.62
Caput caudate nucleus	816 (±114)	936 (±173)	0.08	14.76	0.180 (±0.014)	0.190 (±0.016)	0.21	5.29

studies evaluated the impact of scan parameter on ADC and FA measurements [34–37].

With an increasing number of high field-strength MRI units, DTI is increasingly acquired at 3 Tesla and above. An exact knowledge of the impact of higher field strengths and changes in, e.g., the T2-relaxation on the DTI scalars is mandatory. This is of essential importance when DTI scalars are used in the follow-up of disease processes in which changes in the ADC and FA values might indicate early microstructural disease progression or in cases where measured DTI scalars are compared with normative data. One limitation is that not always can all serial examinations be acquired at the same field strength. Theoretically, DTI scalars should be identical for any used field strength because diffusion is not influenced by the external magnetic field. Several recent studies comparing DTI metrics at different field strengths revealed contradicting findings, however. One recent study concluded that the mean diffusivity and FA did not differ significantly comparing 1.5 and 3 Tesla [27], while in another study an inverse relationship between field strength and ADC of cerebral metabolites was observed [28]. In addition, shorter T2 relaxation times at higher field strengths have also been discussed to influence DTI scalars [28].

Our study, measuring 12 healthy volunteers in controlled conditions at 1.5 and 3 Tesla within 2 h, revealed a statistically significant decrease in ADC values comparing 1.5- with 3.0-Tesla MRI systems for both the white and gray matter. Moreover, a statistically significant increase was also seen for FA measurements of the white and gray matter. The degree of ADC change was less pronounced as the degree of FA change. The FA increase was larger for the central gray matter than for the white matter, resulting in a reduced gray versus white matter differentiation. The higher field strength did not show gray versus white matter dissociating effects on the ADC maps.

The explanation for the field-strength-related differences in measured ADC and FA values is challenging. Methodological or intrinsic physical factors related to differences in the design of the DTI sequences, differences in the duration, amplitude and separation of the diffusion gradients or intrinsic differences in the T2-relaxation comparing 1.5 and 3 Tesla experiments seem straightforward to explain measured differences in DTI scalars. However, in our study special care was taken to minimize any methodological factor that could results in methodological differences in measurements. All imaging parameter were as identical as possible for both scanners (identical manufacturer). In addition, the effect of the different field strength on the b-value was controlled by an exact b-matrix calculation. The discrete change of the b-matrix was taken into account in our calculations. The

Table 3 ADC and FA values measured at 3 Tesla using two different echo times (TE=91 ms and TE=125 ms). ADC×10^{-6} mm^2/s; FA are unitless, varying between 0 (maximal isotropic diffusion) and 1 (maximal anisotropic diffusion). Data are presented as mean ± standard deviation A *P* value less than 0.05 was considered to indicate statistically significant difference

3 Tesla	ADC				FA			
	TE=91	TE=125	*P* value	% change	TE=91	TE=125	*P* value	% change
Genu internal capsule	724 (±22)	728 (±25)	0.76	0.51	0.681 (±0.035)	0.679 (±0.045)	0.80	−0.31
Posterior limb internal capsule	702 (±25)	703 (±23)	0.83	0.19	0.722 (±0.020)	0.722 (±0.023)	0.83	0.13
Splenium corpus callosum	647 (±57)	597 (±88)	0.15	−7.74	0.878 (±0.019)	0.903(±0.042)	0.22	2.82
Truncus corpus callosum	789 (±26)	786 (±32)	0.85	−0.40	0.815 (±0.026)	0.833 (±0.015)	0.27	2.24
Centrum semiovale	702 (±20)	696 (±29)	0.23	−0.87	0.619 (±0.055)	0.640 (±0.057)	0.08	3.39
Thalamus	734 (±19)	745 (±31)	0.31	1.57	0.333 (±0.039)	0.348 (±0.025)	0.33	4.58
Caput caudate nucleus	840 (±90)	872 (±116)	0.39	3.84	0.179 (±0.020)	0.197 (±0.028)	0.12	9.88

potential effect of slightly different diffusion times on the measured apparent diffusion tensor was ignored because very discrete. To our knowledge, at diffusion times of 40–80 ms, typical for clinical DTI, the effect of a restricted diffusion reaches a plateau and is consequently neglectable. To avoid concerns related to over- or underestimation of the degree of diffusion anisotropy, we used FA as marker of tissue anisotropy because FA has been shown to be one of the most robust and noise-resistant scalars of diffusion anisotropy [7, 19, 20]. Furthermore, eddy current artifacts were minimized by using a paired, bipolar positive and negative design of diffusion gradients according to the protocol of Reese et al. [29]. They had shown that with this diffusion gradient design, misregistration artifacts due to eddy currents are negligible [29]. Finally, biological factors that could influence the DTI scalars were also kept as identical as possible. The volunteers were scanned at both field strengths within 2 h.

We measured 12 different geometric directions because according to our own experience and multiple previous publications, the estimation of the diffusion tensor is more accurate if a larger number than the minimum of six directions are sampled [38–41]. Accuracy is strongly increasing for the first 20–30 diffusion directions, for higher numbers of sampling directions the effect is less pronounced. Our study was orientated on our standard clinical protocol that uses 12 directions. By using 12 diffusion encoding directions we anticipated to be sensitive enough to identify small differences in DTI scalars comparing 1.5- with 3-Tesla field strength.

Diffusion in the brain is in general not mono-exponential. However, for b values up to 1,000 s/mm^2 diffusion is considered mono-exponential. Consequently, using the applied DTI sequence, a two-point mono-exponential fit approach gives reliable DTI scalars. In addition, a previous study showed that for a mono-exponential fit, it is more efficient to apply multiple averages at low and high b values rather than to perform measurements with multiple, different b values [38, 42]. Diffusion-weighted MR images are, as a rule, maps of the MR signal magnitude. Therefore, even for a white noise the mean of the noise signal is a positive value. If the signal intensity approximates the noise level, strong errors in the fit will arise [43]. However, in our study the SNR of the diffusion weighted images were at least ten times larger than the noise level and consequently this effect is insignificant.

Magnetic-field-related differences in the SNR could also be causative for the observed differences in DTI metrics. Theoretically, low FA values are expected for brain areas that have a predominant cellular architecture (central gray matter); high FA-values are expected for brain areas with tightly packed fiber tracts (central white matter). Measurements of diffusion anisotropy are known to be highly noise dependent, especially in areas of low anisotropy where the ratio between the magnitude of the principal eigenvectors of the diffusion tensor and the background tissue noise is less favorable [7, 19, 34, 44]. Higher field strengths typically boost the SNR [44]. The field-strength-related SNR gain we observed was in the range of 20% comparing 1.5 with 3.0 Tesla. This is less than the observed 48% reported by Kuhl et al. [45] and 40% reported by Hunsche et al. [27]. This discrepancy might be related to hardware differences and most probably to different RF coil efficiencies. The SNR gain further depends on the applied imaging parameter; in particular on TE. Signal relaxation is more pronounced for TE>T2, as it is the case on the 3.0-Tesla systems. Thus, the different TEs used in our study (91 ms) and that of Kuhl et al. [45] (82 ms) already accounts for approximately 8% difference in SNR gain. With the higher SNR we expect to measure more accurate FA values with higher field strength. This would also explain the differences between the degree of FA change of gray (+11.15%) and white matter (+5.05%). Anatomical areas with a lower degree of anisotropy are more susceptible for background noise contamination and would consequently benefit more from an increased signal as areas that are less susceptible to noise contamination. However, a previous study of Pierpaoli and Basser [19] showed that simulated values of rotationally invariant anisotropy indices like fractional anisotropy (FA) decrease with higher SNR ratios as generated by Monte Carlo methods. They performed a simulation with five different levels of diffusion anisotropy, spanning the range of eigen values observed in brain tissue. The contradiction of Pierpaolo and Basser's findings of a decreasing FA index for higher SNR ratios and our findings of higher FA indices with a higher SNR ratio indicate that the difference in SNR ratio cannot be causative for the measured differences.

Previous studies showed that the T2 relaxation time of gray and white matter decreases with the magnetic field strength [44]. To evaluate the impact of these differences in T2-relaxation times, we compared identical DTI sequences at different echo times for both field strengths. Our results showed that neither at 1.5 Tesla nor at 3.0 Tesla did a statistically significant change in diffusion tensor scalars (ADC and FA) occur. However, due to safety limitations on clinical scanners, the minimal available TE was in the range of (at 1.5 Tesla) or longer (at 3 Tesla, where T2 is in range 39–70 ms) than T2 [46]. This results in a much stronger T2-weighting of DT images at 3 Tesla. Varying TE between 91 and 125 ms may not show a significant effect on the DTI parameters because of small changes in the ratio of the long T2 compartment, while the short T2 compartment has already vanished near complete. That could be an explanation for the observed differences of DTI measurements for the different field strength. To prove this hypothesis DTI measurements need to be done using TEs shorter than those available on clinical scanners.

Major limitation of our study is the relatively small number of subjects that were measured. An additional problem is the lack of a reliable motion correction tool. The inherent differences in signal intensities and contrast on the

diffusion weighted images within one series of diffusion encoding is challenging for any kind of automated motion correction. In addition, our study only compares DTI scalars at two different field strengths. Studies measuring diffusion tensor scalars at multiple field strengths could possibly reveal the exact mathematical relationship between diffusion scalars and field strength. Finally, more extensive comparative studies evaluating the impact of the SNR on diffusion scalars are necessary to give more insight in the relationship between differences in SNR due to a higher magnetic field strength and diffusion scalars.

In summary, our study showed lower ADC and higher FA values at higher field strengths comparing 1.5 with 3.0 Tesla. The importance of this finding for the use of normative diffusion scalars in clinical routine and comparative follow up studies is evident. Our results show that in clinical studies ADC and FA values should be compared with normative values that have been determined at the same field strength as the clinical study has been performed. The exact reason for the observed differences could not (yet) be identified. Possibly, field-dependent differing T2-relaxation times could be causative. Studies on experimental scanners should be performed that allow the use of smaller echo times.

References

1. Le Bihan D, Breton E, Syrota A (1985) Imagerie de diffusion par résonance magnétique nucléaire. C R Acad Sci [III] 301:1109–1112
2. Le Bihan D, Breton E, Lallemand D, Aubin ML, Vignaud J, Laval-Jeantet M (1988) Separation of diffusion and perfusion in intravoxel incoherent motion (IVIM) MR imaging. Radiology 168:497–505
3. Le Bihan D, Turner R, Pekar J, Moonen CTW (1991) Diffusion and perfusion imaging by gradient sensitization: design, strategy and significance. J Magn Reson Imaging 1:7–28
4. Le Bihan D (1990) Diffusion/perfusion MR imaging of the brain: from structure to function. Radiology 177: 328–329
5. Sorensen AG, Buonanno FS, Gonzalez RG, Schwamm LH, Lev MH, Huang-Hellinger FRH, Reese TG, Weiskoff RM, Davis TL, Suwanwela N, Can U, Moreira JA, Copen WA, Look RB, Finkelstein SP, Rosen BR, Koroshetz WJ (1996) Hyperacute stroke: evaluation with combined multislice diffusion-weighted and hemodynamically weighted echo-planar MR imaging. Radiology 199:391–401
6. Lovblad KO, Baird AE, Schlaug G, Benfield A, Siewert B, Voetsch B, Connor A, Burzynski C, Edelman RR, Warach S (1997) Ischemic lesion volumes in acute stroke by diffusion-weighted magnetic resonance imaging correlate with clinical outcome. Ann Neurol 42:164–170
7. Sorensen AG, Wu O, Copen WA, David TS, Gonzalez RG, Koroshetz WJ, Reese TG, Rosen BR, Wedeen VJ, Weiskoff RM (1999) Human acute cerebral ischemia: Detection of changes in water diffusion anisotropy by using MR imaging. Radiology 212:785–792
8. Ciccarelli O, Werring DJ, Wheeler-Kingshott CA, Barker GJ, Parker GJ, Thompson AJ, Miller DH (2001) Investigation of MS normal-appearing brain by using diffusion tensor MRI with clinical correlations. Neurology 56:926–933
9. Werring DJ, Clark CA, Barker GJ, Thompson AJ, Miller DH (1999) Diffusion tensor imaging of lesions and normal-appearing white matter in multiple sclerosis. Neurology 52: 1626–1632
10. Filippi M, Iannuci G, Cercignani M, Rocca MA, Pratesi A, Comi G (2000) A quantitative study of water diffusion in multiple sclerosis lesions and normal-appearing white matter using echo-planar imaging. Arch Neurol 57: 1017–1021
11. Melhem RI, Mori S, Eichler FS, Raymond GV, Moser HW (2001) Diffusion tensor brain MR imaging in X-linked cerebral adrenoleukodystrophy. Neurology 56:544–547
12. Hanyu H, Sakurai H, Iwamoto T, Takasaki M, Shindo H, Abe K (1998) Diffusion-weighted MR imaging of the hippocampus and temporal white matter in Alzheimer's disease. J Neurol Sci 156:195–200
13. Ellis CM, Simmons A, Jones DK, Bland J, Dawson JM, Horsfield MA, Williams SC, Leigh PN (1999) Diffusion tensor MRI assesses corticospinal tract damage in ALS. Neurology 53:1051–1058
14. Pomara N, Crandall DT, Choi SJ, Johnson G, Lim KO (2001) White matter abnormalities in HIV-1 infection: a diffuse tensor imaging study. Psychiatry Res 28:15–24
15. Filippi CG, Ulug AM, Ryan E, Ferrando SJ, Van Gorp W (2001) Diffusion tensor imaging of patients with HIV and normal-appearing white matter on MR images of the brain. AJNR Am J Neuroradiol 22:277–283
16. Maier JF, Clark CA, Barker GJ, Miller DH, Ron MA (2000) Neuropathological abnormalities of the corpus callosum in schizophrenia: a diffusion tensor imaging study. J Neurol Neurosurg Psychiatry 68:242–244
17. Dumas de la Roque A, Oppenheim C, Classoux F et al (2005) Diffusion tensor imaging of partial intractable epilepsy. Eur Radiol 15:279–285
18. Price SJ, Pena A, Burnet NG et al (2004) Tisue signature characterisation of diffusion tensor abnormalities in cerebral gliomas. Eur Radiol 14: 1909–1917
19. Pierpaoli C, Basser PJ (1996) Toward a quantitative assessment of diffusion anisotropy. Magn Reson Med 36: 893–906
20. Pierpaoli C, Jezzard P, Basser PJ, Barnett A, Di Chiro G (1996) Diffusion tensor MR imaging of the human brain. Radiology 201:637–648
21. Shimanoy JS, McKinstry RC, Akbudak E, Aronovitz JA, Snyder AZ, Lori NF, Cull TS, Conturo TE (1999) Quantitative diffusion-tensor anisotropy brain MR imaging: normative human data and anatomic analysis. Radiology 212:770–784

22. Schneider JF, Il'yasov KA, Boltshauser E, Hennig J, Martin E (2003) Diffusion tensor imaging in cases of adrenoleukodystrophy: preliminary experience as a marker for early demyelination? AJNR Am J Neuroradiol 24:819–824
23. Neil JJ, Shiran SI, McKinstry RC, Schefft GL, Snyder AZ, Almli CR, Akbudak E, Aronovitz JA, Miller JP, Lee BCP, Conturo TE (1998) Normal brain in human newborns: apparent diffusion coefficient and diffusion anisotropy measured by using diffusion tensor MR imaging. Radiology 209:57–66
24. Nusbaum AO, Tang CY, Buchsbaum MS, Wei TC, Atlas SW (2001) Regional and global changes in cerebral diffusion with normal aging. AJNR Am J Neuroradiol 22:136–142
25. Schmithorst VJ, Wilke M, Dardzinski BJ, Holland SK (2002) Correlation of white matter diffusivity and anisotropy with age during childhood and adolescence: a cross-sectional diffusion-tensor MR imaging study. Radiology 222:212–218
26. Schneider JFL, Il'yasov KA, Hennig J, Martin E (2004) Fast quantitative diffusion-tensor imaging of cerebral white matter from the neonatal period to adolescence. Neuroradiology 46: 258–266
27. Hunsche S, Moseley ME, Stoeter P, Hedehus M (2001) Diffusion-tensor MR imaging at 1.5 and 3.0 T: initial observations. Radiology 221:550–556
28. Guilfoyle DN, Suckow RF, Baslow MH (2003) The apparent dependence of the diffusion coefficient of N-acetylaspartate upon magnetic field strength: evidence of an interaction with NMR methodology. NMR Biomed 16:468–474
29. Reese TG, Heid O, Weisskoff RM, Wedeen VJ (2003) Reduction of eddy-current-induced distortion in diffusion MRI using a twice-refocused spin echo. Magn Reson Med 49:177–182
30. Il'yasov KA, Barta G, Kreher BW, Bellemann ME, Hennig J (2005) Importance of exact b-tensor calculation for quantitative diffusion tensor imaging and tracking of neuronal fiber bundles. Appl Magn Reson 29 107–122
31. Il'Yasov KA, Hennig J (1998) Single-shot diffusion-weighted RARE sequence: application for temperature monitoring during hyperthermia session. J Magn Reson Imaging 8: 1296–1305
32. Basser PJ, Pierpaoli C (1996) Microstructural and physiological features of tissue elucidated by quantitative-diffusion-tensor MRI. J Magn Reson B 111: 209–219
33. Holz M, Heil SR, Sacco A (2000) Temperature-dependent self-diffusion coefficients of water and six selected molecular liquids for calibration in accurate 1H NMR PFG measurements. Phys Chem 2:4740–4742
34. Melhem ER, Itoh R, Jones L, Barker PB (2000) Diffusion tensor MR imaging of the brain: Effect of diffusion weighting on trace and anisotropy measurements. AJNR Am J Neuroradiol 21:1813–1820
35. Delano MC, Cooper TG, Siebert JE, Potchen MJ, Kuppusamy K (2000) High-b-value diffusion-weighted MR imaging of adult brain: image contrast and apparent diffusion coefficient map features. AJNR Am J Neuroradiol 21:1830–1836
36. Yoshiura T, Wu O, Zaheer A, Reese RG, Sorensen AG (2001) Highly diffusion-sensitized MRI of the brain: dissociation of gray and white matter. Magn Reson Med 45:734–740
37. Burdette JH, Durden DD, Elster AD, Yen YF (2001) High b-value diffusion-weighted MRI of normal brain. J Comput Assist Tomogr 25:515–519
38. Jones DK, Horsfield MA, Simmons A (1999) Optimal strategies for measuring diffusion in anisotropic systems by magnetic resonance imaging. Magn Reson Med 42:515–525
39. Papadakis NG, Xing D, Huang L-H, Hall LD, Carpenter TA (1999) A comparative study of acquisition schemes of diffusion tensor imaging using MRI. J Magn Reson 132:67–82
40. Skare S, Hedehus M, Moseley ME, Li T-Q (2000) Condition number as a measure of noise performance of diffusion tensor data acquisition schemes with MRI. J Magn Reson 147:340–352
41. Batchelor PG, Atkinson D, Hill DL, Calamante F, Connelly A (2003) Anisotropic noise propagation in diffusion tensor MRI sampling schemes. Magn Reson Med 49:1143–1151
42. Conturo TE, McKinstry RC, Aronovitz JA, Neil JJ (1995) Diffusion MRI: precision, accuracy and flow effects. NMR Biomed 8:307–332
43. Dietrich O, Heiland S, Sartor K (2001) Noise correction for the exact determination of apparent diffusion coefficients at low SNR. Magn Reson Med 45: 448–453
44. Crooks LE, Arakawa M, Hoenninger J, McCarten B, Watts J, Kaufman L (1984) Magnetic resonance imaging: effects of magnetic field strength. Radiology 151:127–133
45. Kuhl Ch, Textor J, Gieseke J et al (2005) Acute and subacute ischemic stroke at high-field strength (3.0-T) diffusion-weighted MR imaging: intraindividual comparative study. Radiology 234:509–516
46. Gelman N, Gorell JM, Barker PB et al (1999) MR Imaging of human brain at 3.0 T: preliminary report on transverse relaxation rates and relation to estimated iron content. Radiology 210:759–767